Current Biology 24, 2533–2540, November 3, 2014 ©2014 Elsevier Ltd All rights reserved http://dx.doi.org/10.1016/j.cub.2014.08.066

Report

GMF Promotes Leading-Edge Dynamics and Collective Cell Migration In Vivo

Minna Poukkula,[1] Markku Hakala,[1] Nalle Pentinmikko,[1] Meredith O. Sweeney,[2] Silvia Jansen,[2] Jaakko Mattila,[1,3] Ville Hietakangas,[1,3] Bruce L. Goode,[2] and Pekka Lappalainen[1,*]

[1]Institute of Biotechnology, University of Helsinki, P.O. Box 56, 00014 Helsinki, Finland

[2]Rosenstiel Center for Basic Biomedical Research, Brandeis University, Waltham, MA 02453, USA

[3]Department of Biosciences, University of Helsinki, P.O. Box 56, 00014 Helsinki, Finland

Summary

Lamellipodia are dynamic actin-rich cellular extensions that drive advancement of the leading edge during cell migration [1–3]. Lamellipodia undergo periodic extension and retraction cycles [4–8], but the molecular mechanisms underlying these dynamics and their role in cell migration have remained obscure. We show that glia-maturation factor (GMF), which is an Arp2/3 complex inhibitor and actin filament debranching factor [9, 10], regulates lamellipodial protrusion dynamics in living cells. In cultured S2R$^+$ cells, GMF silencing resulted in an increase in the width of lamellipodial actin filament arrays. Importantly, live-cell imaging of mutant *Drosophila* egg chambers revealed that the dynamics of actin-rich protrusions in migrating border cells is diminished in the absence of GMF. Consequently, velocity of border cell clusters undergoing guided migration was reduced in *GMF* mutant flies. Furthermore, genetic studies demonstrated that GMF cooperates with the *Drosophila* homolog of Aip1 (*flare*) in promoting disassembly of Arp2/3-nucleated actin filament networks and driving border cell migration. These data suggest that GMF functions in vivo to promote the disassembly of Arp2/3-nucleated actin filament arrays, making an important contribution to cell migration within a 3D tissue environment.

Results and Discussion

Branched actin filament networks nucleated by the Arp2/3 complex provide force for many cellular processes involving membrane dynamics. Assembly of branched actin networks is tightly controlled by a variety of Arp2/3 activators, whereas their disassembly is driven through filament severing induced by actin-depolymerizing factor (ADF)/cofilin together with Aip1 and cyclase-associated protein [11–14]. Furthermore, a structural homolog of ADF/cofilin, glia-maturation factor (GMF), inhibits nucleation by the Arp2/3 complex and can prune Arp2/3-nucleated filament networks in vitro to enhance their disassembly [9, 10]. GMF does not interact with actin filaments by itself, but instead binds with high affinity to the interface between Arp2 and the first actin subunit of the daughter filament to sever the branch junction [15, 16]. Studies on cultured mammalian cell lines have suggested that GMF associates with membrane ruffles and contributes somehow to cell migration [17–19]. However, relatively little is known about the in vivo role of GMF in regulating actin dynamics. Studies in yeast have shown that *GMF* displays synthetic genetic interactions with certain *cofilin* mutants, indicating that it may promote actin filament disassembly together with cofilin [9, 10]. Knockdown studies on cultured mammalian cells suggested that GMF promotes the assembly of actin-rich lamellipodia in neutrophils, but functions as a negative regulator of actin polymerization and contraction in human airway smooth muscle cells [18, 20].

To determine the physiological function of GMF in animals and to elucidate its role in regulating dynamics of different actin filament structures in vivo, we applied *Drosophila* as a model system. As mentioned above, two biochemical activities have been reported for GMF, common to both yeast and mouse homologs: inhibition of actin nucleation by Arp2/3 and debranching of daughter filaments from their mothers [9, 10, 15]. We first tested whether *Drosophila* GMF (dGMF) shares these activities. To examine whether GMF affects Arp2/3-mediated actin nucleation, we performed pyrene-actin assembly assays. dGMF at 2 μM inhibited actin nucleation by bovine Arp2/3 complex and human WAVE2 glutathione S-transferase (GST)-verprolin central acidic (VCA) to a similar extent as 2 μM mouse GMFγ (mGMFγ) (Figure 1A). These inhibitory effects of dGMF on nucleation were concentration dependent (Figures 1B and 1C), reaching half-maximal activity at 2–4 μM dGMF, similar to mGMFγ [15]. Furthermore, to monitor filament debranching, we used total internal reflection fluorescence (TIRF) microscopy, and we observed that 500 nM dGMF produced a debranching rate of $1.3 \times 10^{-3} \pm 1.3 \times 10^{-4}$ s^{-1}, similar to the recently measured debranching rate of mGMFγ (about 1.5×10^{-3} s^{-1}) [15] (Figures 1D and 1E; Movie S1 available online). Interestingly, bovine Arp2/3 complex assembles branched actin filaments that have a relatively high rate of spontaneous debranching (6.9×10^{-4} s^{-1} ± 1.2×10^{-4} s^{-1}), in the absence of GMF, compared to the branched filaments produced by yeast Arp2/3 complex, which rarely debranch in the absence of GMF [9]. However, additional Arp2/3 complex-associated factors found in mammalian cells may stabilize branch junctions against spontaneous dissociation until GMF arrives to promote debranching.

In order to study the function of GMF in *Drosophila* cells, we generated a polyclonal antibody that specifically recognizes dGMF. Western blotting and immunostaining revealed that dGMF is expressed in S2R$^+$ cells plated on concanavalin A and partially colocalizes with F-actin to lamellipodia (Figures 1F, 1G, and S1A). In addition, GMF localized to actin-rich ridges at the cell periphery, to perinuclear region, and to the nucleus in cultured *Drosophila* and mammalian cells (Figures 1G, S1A, and S1C; data not shown). These are likely to represent true subcellular localizations of GMF, because similar patterns were also detected with GFP-tagged fusion protein, and because RNAi-mediated silencing caused disappearance of GMF staining at these regions. dGMF localization to the cell edge was prominent in cells displaying a narrow lamellipodia, while in cells with wide lamellipodial actin arrays dGMF did not clearly accumulate along the cell edges (Figure S1A). Furthermore, in cultured *Drosophila* S2 and mouse B16 cells, GFP-GMF was virtually absent from extending lamellipodia, but

*Correspondence: pekka.lappalainen@helsinki.fi

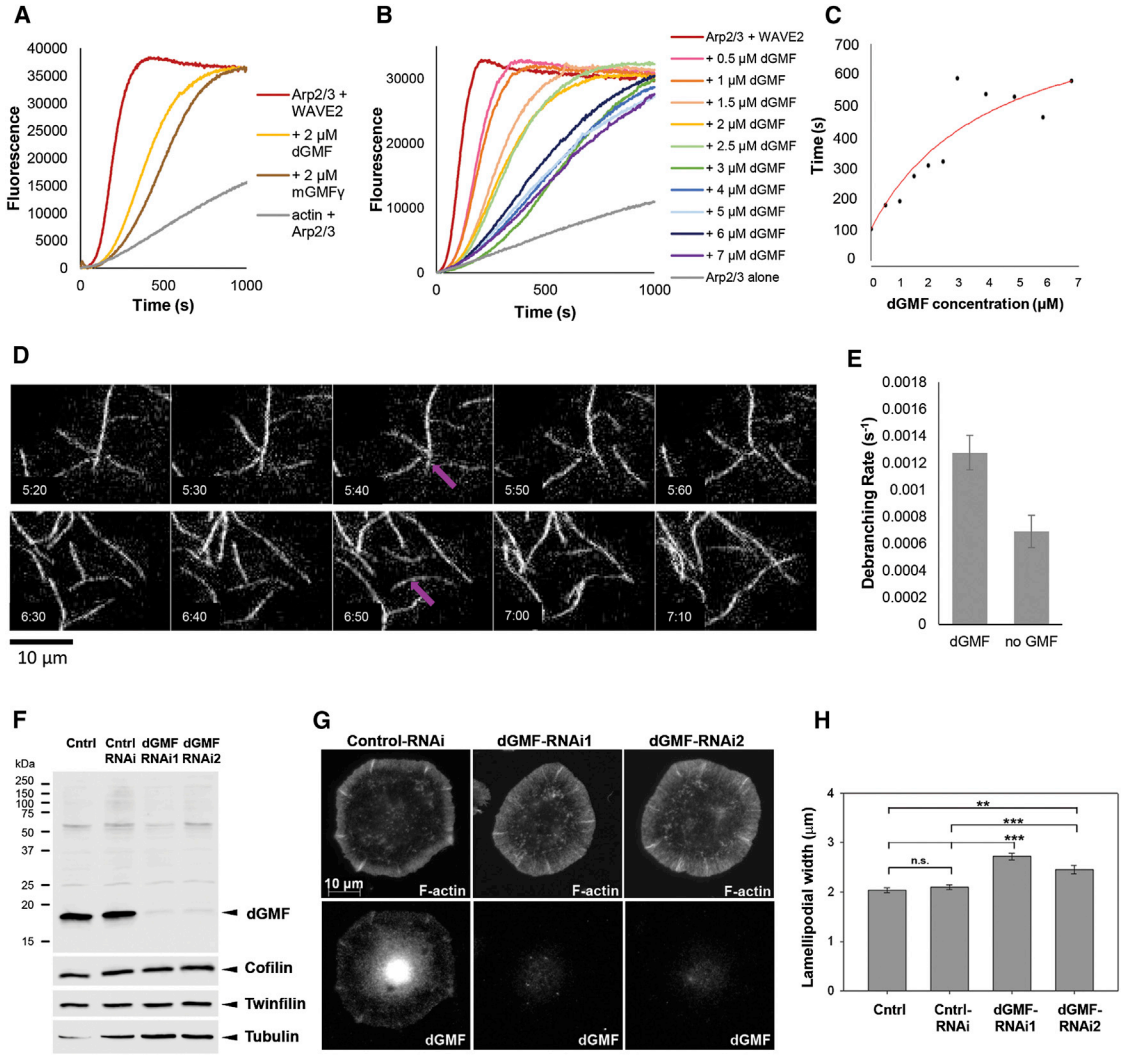

Figure 1. *Drosophila* GMF Inhibits Arp2/3 Complex-Mediated Actin Assembly, Promotes Filament Debranching, and Enhances Disassembly of Lamellipodial Actin Filament Networks

(A) Inhibition of Arp2/3 complex-mediated actin assembly by dGMF and mGMFγ. Reactions contained 2 μM actin monomers (5% pyrene labeled), and as indicated, one or more of the following: 20 nM bovine Arp2/3 complex, 200 nM human WAVE2 GST-VCA, 2 μM dGMF, 2 μM GMFγ.

(B) Effects of different concentrations of dGMF (0–7 μM) in reactions as above.

(C) Concentration-dependent effects of dGMF. Time to half-maximal polymerization for each curve in (B) was measured, and the values are plotted versus dGMF concentration.

(D) TIRF microscopy analysis of filament debranching. Two examples of debranching events observed over time in reactions containing 1 μM actin monomers (10% Oregon green labeled), 5 nM bovine Arp2/3 complex, 100 nM bovine N-WASP GST-VCA, and 500 nM dGMF. Frames were captured at 10 s intervals with 200 ms exposure time. Debranching events are marked by purple arrows.

(E) Data as in (D) were used to calculate debranching probabilities. Data from three different TIRF experiments were averaged. Error bars show SEM.

(F) Western blot analysis of control and dGMF dsRNA-treated S2R$^+$ cell lysates. Western blot shows efficient silencing of dGMF without effects on the expression other ADF-H domain proteins twinfilin and cofilin. Tubulin was used as a loading control.

(G) Control and dGMF knockdown S2R$^+$ cells plated in concanavalin A and stained with anti-dGMF antibody and phalloidin to visualize F-actin. dGMF was enriched in cell edges in control S2R$^+$ cells. Scale bar, 10 μm.

(H) Bar graph presents mean widths of F-actin-rich lamellipodia in control (n = 91), control RNAi (n = 108), dGMF-RNAi1 (n = 96), and dGMF-RNAi2 (n = 114) cells. Data shown indicate mean ± SEM. The differences between the widths of lamellipodia in dGMF-silenced cells and controls are statistically significant, while the differences with control and control RNAi are not. ***p < 0.001, **p < 0.01, Student's t test.

See also Figure S1 and Movie S1.

appeared to enrich in lamellipodia specifically during the retraction phase. This is because GMF intensity increased in lamellipodia by ~2-fold during the retraction phase, whereas mCherry-actin displayed only an ~1.5-fold increase in the intensity during this period (Figures S1B–S1E). However, apparent enrichment of GMF at this stage may at least partially result from increased thickness of retracting lamellipodia; thus, further studies are required to reveal whether GMF localization to Arp2/3-containing actin structures is indeed temporally regulated during lamellipodia extension-retraction. Importantly, silencing of dGMF by two independent double-stranded RNAs (dsRNAs) resulted in a significant increase in the width of lamellipodial actin filament arrays in S2R$^+$ cells, demonstrating that dGMF is either a negative regulator of actin

filament assembly or a promoter of the disassembly of actin filament arrays in cultured cells (Figures 1G and 1H).

The localization and function of GMF in S2 cells prompted us to study its function during border cell migration in the *Drosophila* ovary, because it is a well-established genetic model for directed cell migration in vivo [21, 22]. A group of border cells delaminates from the follicular epithelium during stage 9 of oogenesis and performs stereotypical migration between nurse cells to the oocyte. During this collective migration, border cells extend dynamic actin-rich cellular protrusions [23–26]. Mutations in actin regulators, such as cofilin, profilin, and the small GTPase Rac, cause border cell migration delays, demonstrating that precise regulation of actin cytoskeleton dynamics is required for migration [27–30]. Immunostaining of ovaries showed that dGMF is expressed in the follicular epithelium and is more prominent in polar cells, migrating border cells, and centripedal cells (Figures 2A and 2B; unpublished data). To examine the role of dGMF in border cell migration, we generated a *dGMF* mutant allele by imprecise excision of P element P{EP}CG5869(G2885). One mutant allele, gmf^{1}, which lacked entire coding region of *dGMF* and part of the neighboring gene *CG17328*, was recovered (Figure 2C). Western blot and immunostaining analyses of flies and their ovaries demonstrated that the gmf^{1} mutant did not express dGMF protein (Figure 2D; data not shown). The gmf^{1} mutants were viable and fertile and did not show obvious developmental phenotypes. In addition, when analyzed from fixed samples of stage 10 egg chambers, border cell migration in gmf^{1} mutants was not severely compromised compared to wild-type cells (Figures 2E and 2F). Furthermore, overexpression of GMF in flies did not result in obvious defects in viability, bristle morphogenesis, or border cell migration (Figures S2A–S2C).

Because border cells were able to reach their final destination in the egg chamber at stage 10 in gmf^{1} mutant flies, we examined possible genetic interactions between *GMF* and other regulators of actin filament disassembly. These experiments revealed that lack of dGMF displays strong synergistic effects in border cell migration with the cofilin cofactor Aip1. This protein promotes rapid actin turnover by interacting with cofilin-decorated actin filaments and enhancing their disassembly [12, 31–33]. In *Drosophila*, inactivation of the Aip1 homolog *Flare* causes defects similar to cofilin (*Twinstar*) mutants, including accumulation of excess F-actin and increased stability of actin networks [34, 35]. Our experiments revealed that Aip1 silencing caused F-actin accumulation and moderate border cell migration delays as detected from fixed stage 10 egg chambers. However, in the gmf^{1} mutant background actin accumulation and cell migration delay were strongly enhanced, with the majority of border cell clusters failing to properly delaminate from the epithelium or remaining at the anterior tip of the egg chamber (Figures 2E and 2F). Similar genetic interactions were observed when dGMF was depleted from ovaries by RNAi (Figure S2D). Simultaneous inactivation of dGMF and Aip1 also resulted in an accumulation of F-actin in follicular epithelium of developing egg chambers, and in deformation of bristles in the thorax (Figures S2E–S2G).

Because debranching of Arp2/3-nucleated actin filaments is a conserved activity of GMFs in vitro, we examined whether dGMF localizes specifically to Arp2/3-nucleated actin filament structures in vivo and whether lack of dGMF induces defects in the disassembly of Arp2/3-nucleated actin filament networks. As a marker of the Arp2/3 complex, we expressed GFP-tagged Arcp1/p40 (actin-related protein 2/3 complex, subunit 1; aka Sop2) in border cells [36]. Aip1 silencing in border cells resulted in accumulation of F-actin dots, which were often enriched with Arcp1-GFP and dGMF. Simultaneous silencing of Aip1 and dGMF enhanced the accumulation of F-actin foci, which were marked by Arcp1-GFP (Figure 2G). To reveal whether GMF specifically localizes to actin filament arrays nucleated by Arp2/3 complex, we also examined dGMF distribution in follicular epithelium expressing constitutively active actin filament nucleator Dia1 formin that promotes formation of straight actin filaments independently of Arp2/3. Importantly, although Dia1 expression led to the appearance of F-actin-rich foci in cells, dGMF was not enriched on these structures (Figure 2H). These observations suggest that dGMF localizes specifically to Arp2/3-nucleated actin arrays in animal tissues and promotes their disassembly together with Aip1.

To confirm the role of Aip1 and GMF in the disassembly of Arp2/3-nucleated actin filament networks, we silenced Aip1 and GMF in *Drosophila* $S2R^{+}$ cells. As we observed in border cells in vivo, simultaneous depletion of Aip1 and dGMF in $S2R^{+}$ cells resulted in F-actin accumulation, seen as cytoplasmic aggregates, as well as in thickening of lamellipodial actin-rich ridges (Figure 3). Importantly, formation of these actin aggregates was Arp2/3 dependent, because silencing of ArpC5/p16, a component of Arp2/3 complex, prevented F-actin accumulation upon GMF and Aip1 depletion. As reported previously [37], Arp2/3 inhibition in S2 cells led to a spiky phenotype, reflecting the inability to nucleate new cortical actin filaments. Simultaneous silencing of Aip1 and GMF failed to induce formation of abnormal actin filament aggregates in these cells (Figures 3A and 3B).

To further investigate how GMF and Aip1 cooperate in promoting disassembly of Arp2/3-nucleated actin networks, we monitored Arp2/3 nucleation inhibition and debranching using pyrene actin filament disassembly and TIRF assays, respectively (Figure S3). Although dGMF and Aip1 function synergistically in vivo, Aip1 did not enhance GMF activities in vitro, suggesting that these two proteins are unlikely to directly collaborate in promoting actin filament disassembly. Instead, the cooperative effects observed in vivo are likely due to separate, complementary roles in promoting actin disassembly in cooperation with cofilin (i.e., GMF promotes the disassembly of actin networks by enhancing filament debranching and inhibiting nucleation by Arp2/3 complex, whereas Aip1 enhances cofilin-mediated filament severing). In budding yeast, GMF displays synthetic genetic interaction with cofilin [9]. However, because cofilin depletion resulted in lethal phenotype in flies, genetic interactions between GMF and cofilin could not be examined in this system.

Because our genetic analysis of GMF and Aip1 indicated that dGMF indeed contributes to border cell migration, we examined in more detail the role of dGMF during this process by performing live-cell imaging of *Drosophila* egg chambers. In these experiments, border cells were visualized by expression of actin-GFP, and the plasma membranes of the egg chamber cells were labeled with red membrane dye *N*-(3-triethylammoniumpropyl)-4-(6-(4-(diethylamino) phenyl)hexatrienyl)pyridinium dibromide (FM4-64) (Figure 4A). Only posterior migration to the oocyte was analyzed, and this was further divided into early and late migration phases [25, 26]. Early phase was defined as the detachment of border cell cluster from the epithelium and the first 50% of its journey to the oocyte; late phase was defined as the remaining 50% of the journey until border cell clusters contacted the oocyte (Figure 4A). There are changes in the behavior of wild-type border cell clusters during their posterior migration. In the early phase, border

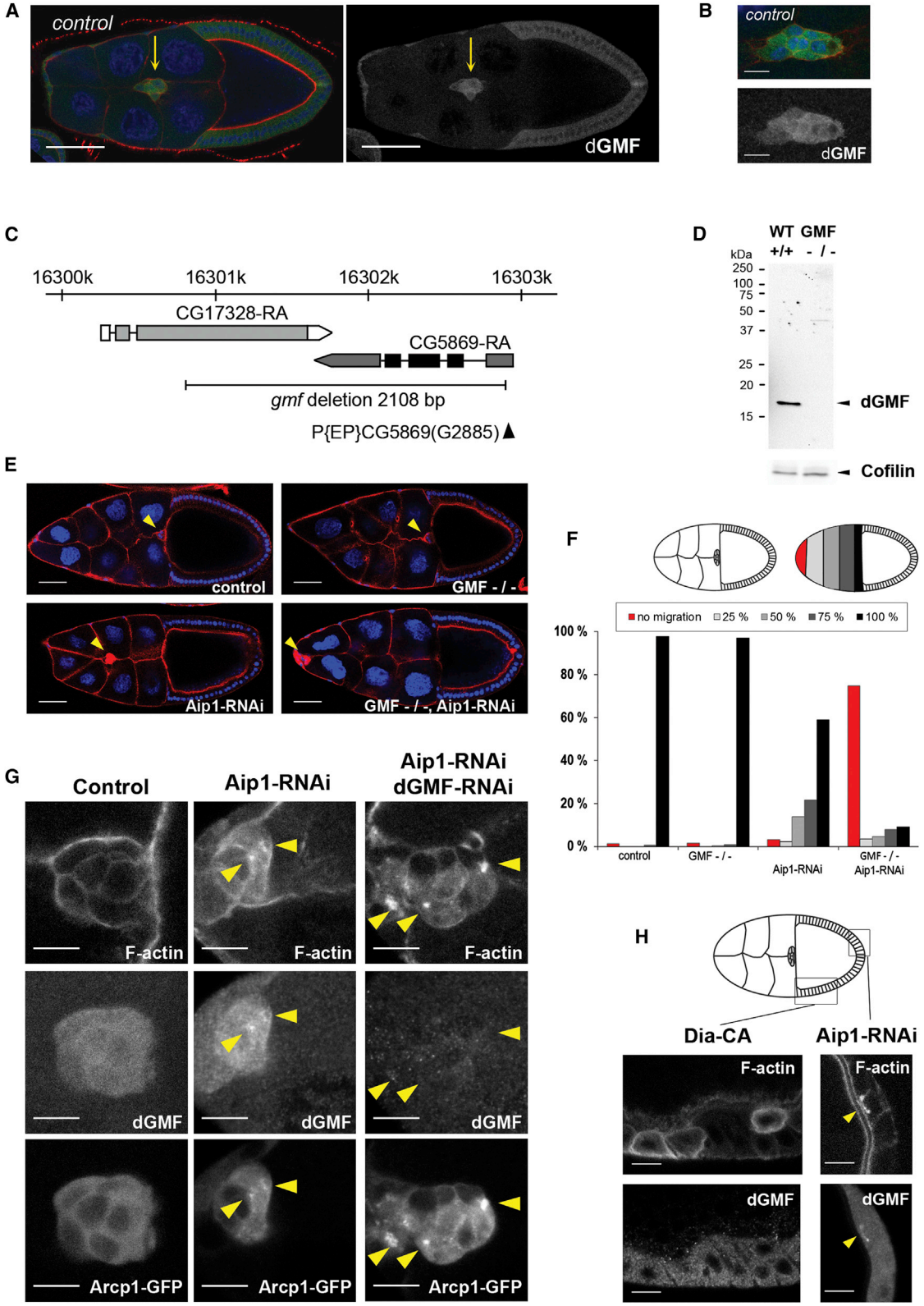

Figure 2. dGMF Is Expressed in Migrating Border Cells and Displays Genetic Interaction with Aip1 to Drive Border Cell Migration and Disassembly of Arp2/3-Nucleated Dendritic F-Actin Networks

(A) A dGMF-specific antibody demonstrates expression of dGMF in migrating border cells. dGMF is shown in green, DAPI (blue) labels DNA, and phalloidin (red) labels F-actin in left panel. Only the dGMF channel is shown in the right panel. Border cells (indicated by arrow) display elevated dGMF expression compared to follicular epithelium. Scale bar, 50 μm. For this and subsequent figures, anterior is on the left.

(B) In migrating border cells, dGMF displays predominantly diffuse cytoplasmic localization. Scale bar, 10 μm. Genotype for (A) and (B) is W1118.

(legend continued on next page)

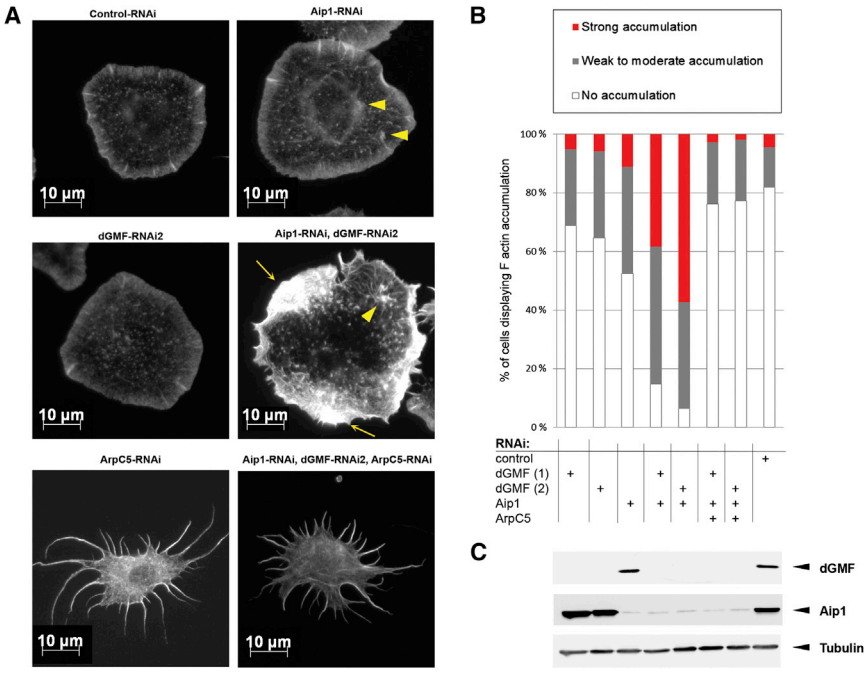

Figure 3. Accumulation of F-Actin in dGMF- and Aip1-Depleted S2R$^+$ Cells Is Dependent on Arp2/3

(A) Accumulation of F-actin aggregates upon silencing of dGMF and Aip1 is blocked by simultaneous depletion of the Arp2/3 complex subunit ArpC5/p16. Control, dGMF, Aip1, ArpC5, dGMF+Aip1, and dGMF+Aip1+ArpC5 knockdown S2R$^+$ cells plated in concanavalin A and stained with phalloidin to visualize F-actin. Arrowheads indicate small actin aggregates in Aip1 and Aip1/dGMF knockdown cells, whereas arrows indicate pronounced F-actin aggregates in Aip1/dGMF knockdown cells. Please note that depletion of ArpC5 results in a spiky phenotype typical for Arp2/3 inhibition [37] both in the presence and absence of Aip1 and GMF.

(B) Bar graph showing percentage of cells with none (white), weak-to-moderate (gray), or strong (red) F-actin accumulation. Samples were scored blindly. n = 105–235.

(C) Western blot analysis of dsRNA-treated S2R$^+$ cell lysates demonstrating efficient silencing of dGMF and Aip1. Tubulin was used as a loading control. Note that the stellate morphology of ArpC5/p16-silenced cells in (A) is similar to that described for silencing of Arp2/3 complex components in S2 cells and thus verifies the efficient silencing of ArpC5/p16.

See also Figure S3.

cell clusters are elongated, and their movement is more streamlined and rapid. This migration phase is characterized by the extension of relatively large front protrusions that are long lived and requires the Rac exchange factors Vav or Elmo/DOCK180 [25, 26]. In the late phase, border cell clusters are more round in shape, their movements are more disordered, and the speed of their migration is approximately half that of the early phase (Figures 4B and 4C; Movie S2) [25, 26]. Although our analysis of border cell migration in fixed samples did not reveal gross defects in *gmf*^{1} mutant flies (Figures 3E and 3F), our live-cell imaging analysis revealed that border cells in *gmf*^{1} mutant flies migrate significantly slower than in wild-type flies, especially during the early phase (Figure 4B; Movie S3). This was indicated by a decrease in the average speed of border cell cluster migration. Despite slower migration speed, *gmf*^{1} mutant border cells finished their migration in time when scored at stage 10, similarly to reported previously for other fly strains with diminished border cell migration speeds (e.g., [26]). Furthermore, decreased single cell speed of *gmf*^{1} mutant border cells demonstrated that, in addition to decreased directionality, individual border cells were less motile compared to wild-type cells during the early phase (Figures 4B and S4A).

We next examined the possible effects of dGMF on the dynamics of cellular extensions in migrating border cells (Figure S4B). Extensions in *gmf*^{1} mutant border cells displayed the front-biased distribution similar to control cells, indicating that border cells were able to read the guidance gradients and that front-back polarity of the border cell cluster was maintained also in the absence of dGMF (Figure S4C). Moreover, *gmf*^{1} mutant border cells were capable of forming extensions in a similar, albeit somewhat decreased amount compared to

(C) Schematic diagram of dGMF (cg5869) chromosomal locus showing the dGMF transcript. P element insertion P{EP}CG5869(G2885) is indicated by black arrowhead. dGMF mutant was generated by imprecise excision, and the black line indicates the 2,108 base pair region deleted in GMF mutant.

(D) Western blot analysis of control (*W1118*) and homozygous dGMF mutant flies using anti-dGMF antibodies. Cofilin was used as a loading control.

(E) Representative images of stage 10 egg chambers. Nuclei are in blue and F-actin is in red. Yellow arrowheads indicate border cell clusters. Scale bar, 50 µm.

(F) Quantification of border cell migration delays in stage 10. Upper panel, left-hand side: schematic presentation of control border cells that have finished their migration to the oocyte. Right-hand side: principles of scoring the position of border cells as a percentage of their migration path to the oocyte: border cell clusters that did not delaminate or migrate (red); that migrated 25% (light gray), 50% (gray), or 75% (dark gray); and finished their posterior migration to the oocyte (black). Lower panel: quantitation of the positions of border cell clusters in stage 10 egg chambers. While wild-type and GMF mutant border cells finish their migration in stage 10, Aip1 silencing causes moderate migration delays and accumulation of F-actin. These abnormalities are strongly enhanced by combining Aip1 silencing and the *gmf*^{1} mutant. n = 87–207.

(G) Accumulation of Arp2/3-enriched F-actin aggregates (yellow arrowheads) in Aip1- and GMF-silenced cells. Aip1 silencing led to formation of small F-actin aggregates in border cells, and >70% of the foci displayed clear accumulation of Arp2/3 and dGMF. Simultaneous silencing of Aip1 and dGMF caused increased intensity and size of F-actin aggregates, virtually all of which were strongly enriched in Arp2/3. F-actin is labeled with phalloidin, endogenous dGMF is stained with an antibody, and Arp2/3 is visualized by Arpc1-GFP fusion. Scale bar, 10 µm. Genotypes for (F) and (G) were c306Gal4/+ (control), c306Gal4/+; *gmf*^{1}/*gmf*^{1} (dGMF$^{-/-}$), c306Gal4/+; +/+; UAS-Aip1-RNAi GD/+ (Aip1-RNAi), and c306Gal4/+; *gmf*^{1}/*gmf*^{1}; UAS-Aip1-RNAi GD/+ (dGMF$^{-/-}$, Aip1-RNAi).

(H) Aip1 silencing resulted in localization of dGMF at sites of F-actin accumulation, whereas dGMF did not localize to F-actin aggregates induced by overexpression of constitutive active formin Dia. Confocal images of follicular epithelium displaying F-actin accumulation (detected by fluorescent phalloidin). Genotypes are c306Gal4/+; UAS-Aip1-RNAi kk/+ (Aip1-RNAi) and UAS-Dia-CA/+; +/SlboGal4 (overexpression of constitutively active Dia). The site of F-actin and dGMF accumulation in Aip1-silenced epithelium is indicated with yellow arrowhead. Scale bar, 10 µm.

See also Figure S2.

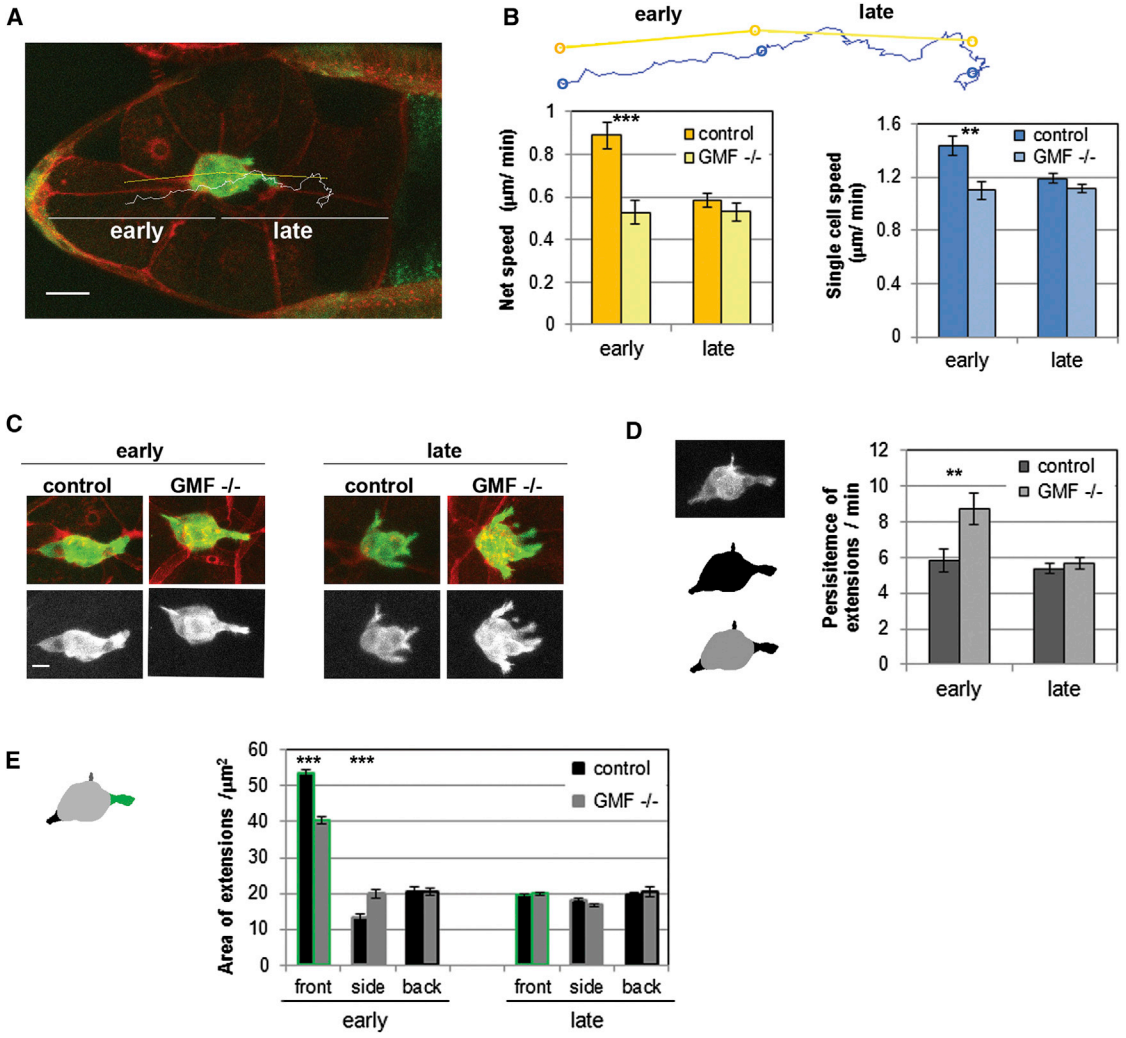

Figure 4. dGMF Promotes the Migration of Border Cells and Increases the Dynamics of Cellular Extensions

(A) Time-lapse image of the egg chamber where border cells have reached 50% of their migration path. Border cells are marked by expression of actin-GFP and the tissue surrounding them with red membrane dye FM4-64. For analysis, the movies were divided into early and late phases according to the time point where border cells first reach 50% of their migration path. Scale bar, 20 μm.

(B) Quantification of net speed (yellow bars) and speed of tracked single cells (blue bars) from live movies. Net speed was calculated based on distance between the start position and end position of the border cluster center (yellow lines). Single cell speed was calculated based on the path that nucleus of a single border cell traveled (white line in A, blue line in B). n = 17–38. Data shown indicate mean ± SEM. ***p < 0.001, **p < 0.01, Student's t test.

(C) Still images from time-lapse movies representing typical morphology of border cell clusters during early and late phases of posterior migration. Scale bar, 10 μm.

(D) Left-hand side: extensions (bottom image, black objects are extensions detected from the macro) of the border cell clusters were extracted from projected 2D GFP-channels (upper image) by using automated macros. Right-hand side: the persistence of extensions in minutes was quantitated by using the customized macros. Data shown indicate mean ± SEM. **p < 0.01, Student's t test.

(E) Average areas of the front, side, and back extensions. For measuring the area of extensions, each time frame was analyzed, and extensions were separated according to their direction into forward (0°–45° and 315°–360°), backward (135°–225°), and sideway (the rest) directions. Data shown indicate mean ± SEM. Genotypes in Figure 4 are 2xsblo-Actin-GFP/+ (control), 2xsblo-Actin-GFP. gmf^{1}/gmf^{1} ($dGMF^{-/-}$).

See also Figure S4 and Movies S2 and S3.

control cells, suggesting that initiation of extensions was not severely compromised in gmf^{1} mutants (Figure S4D). On the other hand, the lifetime of extensions was significantly increased in gmf^{1} mutant border cell clusters during the early phase (Figure 4D). Furthermore, the average areas of the front extensions were decreased and the area of side extensions increased in gmf^{1} mutant border cells (Figure 4E). Thus, gmf^{1} mutant border cells display two different phenotypes in early phase: increased lifetime of extensions and decreased forward-directed protrusion areas. Increased lifetime of extensions suggests that retraction dynamics of extensions is diminished. Decreased protrusion area, in turn, suggests that GMF may promote outgrowth of large productive extensions involved in forward movement. This phenotype may be linked to lack of assembly competent actin monomers, resulting from defects in GMF-mediated actin filament network disassembly, and therefore abnormal stabilization of preexisting protrusions. To elucidate whether the decreased migration speed of gmf^{1} mutant border cells was due to smaller front extensions, we analyzed the forward movement of border cell

clusters normalized by their front extension areas, which revealed that the smaller area of front extensions in *gmf*^{1} mutant border cells correlates well with their slower forward movement (Figures 4B and 4D). Together, these results suggest that dGMF enhances the retraction dynamics of cellular extensions in border cells and thus plays an important role in directional migration of border cell clusters in *Drosophila* egg chambers.

Collectively, our data reveal that in cultured cells and animal tissues GMF localizes to Arp2/3-nucleated actin filament arrays and promotes their disassembly. These results are consistent with genetic interactions between GMF and cofilin mutants in yeast and provide in vivo support for the role of GMF as a debranching factor [9]. Our studies using RNAi silencing and a *gmf*^{1} mutant strain to inactivate dGMF in *Drosophila* tissues revealed that GMF plays an important role in guided, collective cell migration in the tissue environment and cooperates in this process with Aip1. Importantly, live-cell imaging analysis of border cell migration in egg chambers revealed that GMF is required to maintain dynamic cell extensions. Interestingly, lamellipodia in cultured cells display oscillatory behavior consisting of protrusion and retraction periods [8], where Arp2/3 complex is enriched during the extension period [7]. Our work suggests that, reciprocally, GMF is not enriched at the lamellipodium during the extension period. Thus, GMF does not appear to regulate the assembly of Arp2/3-nucleated lamellipodial actin filament arrays, but instead promotes their disassembly to facilitate lamellipodial retraction. In the future, it will be important to elucidate the pathways regulating GMF activity and localization in lamellipodial dynamics. Good candidates for the mechanisms controlling GMF localization and activity in vivo include GMF phosphorylation and nucleotide hydrolysis by Arp2/3 complex. This is because Arp2/3 association of GMF can be regulated by phosphorylation of a serine residue in its N terminus and because GMF preferentially interacts with "aged" ADP-Arp2/3 complex [17, 38]. It will also be important to address the possible interplay between GMF and other negative regulators of Arp2/3 complex, including coronin [39, 40], PICK1 [41], and arpin [42].

Supplemental Information

Supplemental Information includes Supplemental Experimental Procedures, four figures, and three movies and can be found with this article online at http://dx.doi.org/10.1016/j.cub.2014.08.066.

Author Contributions

M.P., M.H., N.P., M.O.S., S.J., J.M., and V.H. performed the experiments and analyzed the data. M.P., V.H., B.L.G., and P.L. designed the study. M.P., B.L.G., and P.L. prepared the manuscript.

Acknowledgments

We thank James Bamburg, Martin Bähler, Jiong Chen, Joseph Dopie, Dyche Mullins, Brad Nolen, Osamu Shimmi, and Maria Vartiainen for sharing reagents and Pernille Rørth and the Bloomington and Vienna RNAi *Drosophila* stock centers for fly strains. We thank the Anna-Liisa Nyfors and Light Microscopy Unit for technical assistance and Casey Ydenberg for assistance in TIRF debranching analysis. This work was supported by grants from the NIH (GM063691) to B.L.G. and ERC (281720) to V.H. and from Biocentrum Helsinki (to P.L.) and the Academy of Finland to M.P. (project 133223) and P.L. (project 251292).

Received: November 26, 2013
Revised: August 1, 2014
Accepted: August 29, 2014
Published: October 9, 2014

References

1. Pollard, T.D., and Borisy, G.G. (2003). Cellular motility driven by assembly and disassembly of actin filaments. Cell *112*, 453–465.
2. Bugyi, B., and Carlier, M.F. (2010). Control of actin filament treadmilling in cell motility. Annu. Rev. Biophys. *39*, 449–470.
3. Ridley, A.J. (2011). Life at the leading edge. Cell *145*, 1012–1022.
4. Giannone, G., Dubin-Thaler, B.J., Döbereiner, H.G., Kieffer, N., Bresnick, A.R., and Sheetz, M.P. (2004). Periodic lamellipodial contractions correlate with rearward actin waves. Cell *116*, 431–443.
5. Weiner, O.D., Marganski, W.A., Wu, L.F., Altschuler, S.J., and Kirschner, M.W. (2007). An actin-based wave generator organizes cell motility. PLoS Biol. *5*, e221.
6. Machacek, M., Hodgson, L., Welch, C., Elliott, H., Pertz, O., Nalbant, P., Abell, A., Johnson, G.L., Hahn, K.M., and Danuser, G. (2009). Coordination of Rho GTPase activities during cell protrusion. Nature *461*, 99–103.
7. Ryan, G.L., Petroccia, H.M., Watanabe, N., and Vavylonis, D. (2012). Excitable actin dynamics in lamellipodial protrusion and retraction. Biophys. J. *102*, 1493–1502.
8. Allard, J., and Mogilner, A. (2013). Traveling waves in actin dynamics and cell motility. Curr. Opin. Cell Biol. *25*, 107–115.
9. Gandhi, M., Smith, B.A., Bovellan, M., Paavilainen, V., Daugherty-Clarke, K., Gelles, J., Lappalainen, P., and Goode, B.L. (2010). GMF is a cofilin homolog that binds Arp2/3 complex to stimulate filament debranching and inhibit actin nucleation. Curr. Biol. *20*, 861–867.
10. Nakano, K., Kuwayama, H., Kawasaki, M., Numata, O., and Takaine, M. (2010). GMF is an evolutionarily developed Adf/cofilin-super family protein involved in the Arp2/3 complex-mediated organization of the actin cytoskeleton. Cytoskeleton (Hoboken) *67*, 373–382.
11. Rotty, J.D., Wu, C., and Bear, J.E. (2013). New insights into the regulation and cellular functions of the ARP2/3 complex. Nat. Rev. Mol. Cell Biol. *14*, 7–12.
12. Okreglak, V., and Drubin, D.G. (2010). Loss of Aip1 reveals a role in maintaining the actin monomer pool and an in vivo oligomer assembly pathway. J. Cell Biol. *188*, 769–777.
13. Normoyle, K.P., and Brieher, W.M. (2012). Cyclase-associated protein (CAP) acts directly on F-actin to accelerate cofilin-mediated actin severing across the range of physiological pH. J. Biol. Chem. *287*, 35722–35732.
14. Chaudhry, F., Breitsprecher, D., Little, K., Sharov, G., Sokolova, O., and Goode, B.L. (2013). Srv2/cyclase-associated protein forms hexameric shurikens that directly catalyze actin filament severing by cofilin. Mol. Biol. Cell *24*, 31–41.
15. Ydenberg, C.A., Padrick, S.B., Sweeney, M.O., Gandhi, M., Sokolova, O., and Goode, B.L. (2013). GMF severs actin-Arp2/3 complex branch junctions by a cofilin-like mechanism. Curr. Biol. *23*, 1037–1045.
16. Luan, Q., and Nolen, B.J. (2013). Structural basis for regulation of Arp2/3 complex by GMF. Nat. Struct. Mol. Biol. *20*, 1062–1068.
17. Ikeda, K., Kundu, R.K., Ikeda, S., Kobara, M., Matsubara, H., and Quertermous, T. (2006). Glia maturation factor-gamma is preferentially expressed in microvascular endothelial and inflammatory cells and modulates actin cytoskeleton reorganization. Circ. Res. *99*, 424–433.
18. Aerbajinai, W., Liu, L., Chin, K., Zhu, J., Parent, C.A., and Rodgers, G.P. (2011). Glia maturation factor-γ mediates neutrophil chemotaxis. J. Leukoc. Biol. *90*, 529–538.
19. Lippert, D.N., and Wilkins, J.A. (2012). Glia maturation factor gamma regulates the migration and adherence of human T lymphocytes. BMC Immunol. *13*, 21.
20. Wang, T., Cleary, R.A., Wang, R., and Tang, D.D. (2014). GMF-γ phosphorylation at Tyr-104 regulates actin dynamics and contraction in human airway smooth muscle. Am. J. Respir. Cell. Mol. Biol. Published online May 12, 2014. http://dx.doi.org/10.1165/rcmb.2014-0125OC.
21. Rørth, P. (2002). Initiating and guiding migration: lessons from border cells. Trends Cell Biol. *12*, 325–331.
22. Montell, D.J. (2003). Border-cell migration: the race is on. Nat. Rev. Mol. Cell Biol. *4*, 13–24.
23. Fulga, T.A., and Rørth, P. (2002). Invasive cell migration is initiated by guided growth of long cellular extensions. Nat. Cell Biol. *4*, 715–719.
24. Prasad, M., and Montell, D.J. (2007). Cellular and molecular mechanisms of border cell migration analyzed using time-lapse live-cell imaging. Dev. Cell *12*, 997–1005.

25. Bianco, A., Poukkula, M., Cliffe, A., Mathieu, J., Luque, C.M., Fulga, T.A., and Rørth, P. (2007). Two distinct modes of guidance signalling during collective migration of border cells. Nature *448*, 362–365.
26. Poukkula, M., Cliffe, A., Changede, R., and Rørth, P. (2011). Cell behaviors regulated by guidance cues in collective migration of border cells. J. Cell Biol. *192*, 513–524.
27. Chen, J., Godt, D., Gunsalus, K., Kiss, I., Goldberg, M., and Laski, F.A. (2001). Cofilin/ADF is required for cell motility during Drosophila ovary development and oogenesis. Nat. Cell Biol. *3*, 204–209.
28. Verheyen, E.M., and Cooley, L. (1994). Profilin mutations disrupt multiple actin-dependent processes during Drosophila development. Development *120*, 717–728.
29. Murphy, A.M., and Montell, D.J. (1996). Cell type-specific roles for Cdc42, Rac, and RhoL in Drosophila oogenesis. J. Cell Biol. *133*, 617–630.
30. Geisbrecht, E.R., and Montell, D.J. (2004). A role for Drosophila IAP1-mediated caspase inhibition in Rac-dependent cell migration. Cell *118*, 111–125.
31. Rodal, A.A., Tetreault, J.W., Lappalainen, P., Drubin, D.G., and Amberg, D.C. (1999). Aip1p interacts with cofilin to disassemble actin filaments. J. Cell Biol. *145*, 1251–1264.
32. Okada, K., Obinata, T., and Abe, H. (1999). XAIP1: a Xenopus homologue of yeast actin interacting protein 1 (AIP1), which induces disassembly of actin filaments cooperatively with ADF/cofilin family proteins. J. Cell Sci. *112*, 1553–1565.
33. Okada, K., Ravi, H., Smith, E.M., and Goode, B.L. (2006). Aip1 and cofilin promote rapid turnover of yeast actin patches and cables: a coordinated mechanism for severing and capping filaments. Mol. Biol. Cell *17*, 2855–2868.
34. Ren, N., Charlton, J., and Adler, P.N. (2007). The flare gene, which encodes the AIP1 protein of Drosophila, functions to regulate F-actin disassembly in pupal epidermal cells. Genetics *176*, 2223–2234.
35. Chu, D., Pan, H., Wan, P., Wu, J., Luo, J., Zhu, H., and Chen, J. (2012). AIP1 acts with cofilin to control actin dynamics during epithelial morphogenesis. Development *139*, 3561–3571.
36. Hudson, A.M., and Cooley, L. (2002). A subset of dynamic actin rearrangements in Drosophila requires the Arp2/3 complex. J. Cell Biol. *156*, 677–687.
37. Kunda, P., Craig, G., Dominguez, V., and Baum, B. (2003). Abi, Sra1, and Kette control the stability and localization of SCAR/WAVE to regulate the formation of actin-based protrusions. Curr. Biol. *13*, 1867–1875.
38. Boczkowska, M., Rebowski, G., and Dominguez, R. (2013). Glia maturation factor (GMF) interacts with Arp2/3 complex in a nucleotide state-dependent manner. J. Biol. Chem. *288*, 25683–25688.
39. Humphries, C.L., Balcer, H.I., D'Agostino, J.L., Winsor, B., Drubin, D.G., Barnes, G., Andrews, B.J., and Goode, B.L. (2002). Direct regulation of Arp2/3 complex activity and function by the actin binding protein coronin. J. Cell Biol. *159*, 993–1004.
40. Cai, L., Makhov, A.M., Schafer, D.A., and Bear, J.E. (2008). Coronin 1B antagonizes cortactin and remodels Arp2/3-containing actin branches in lamellipodia. Cell *134*, 828–842.
41. Rocca, D.L., Martin, S., Jenkins, E.L., and Hanley, J.G. (2008). Inhibition of Arp2/3-mediated actin polymerization by PICK1 regulates neuronal morphology and AMPA receptor endocytosis. Nat. Cell Biol. *10*, 259–271.
42. Dang, I., Gorelik, R., Sousa-Blin, C., Derivery, E., Guérin, C., Linkner, J., Nemethova, M., Dumortier, J.G., Giger, F.A., Chipysheva, T.A., et al. (2013). Inhibitory signalling to the Arp2/3 complex steers cell migration. Nature *503*, 281–284.